Laplacian spectra as a diagnostic tool for network structure and dynamics

Patrick N. McGraw and Michael Menzinger
Department of Chemistry, University of Toronto, Toronto, Ontario, Canada M5S 3H6
(Received 22 August 2007; published 4 March 2008)

We examine numerically the three-way relationships among structure, Laplacian spectra, and frequency synchronization dynamics on complex networks. We study the effects of clustering, degree distribution, and a particular type of coupling asymmetry (input normalization), all of which are known to have effects on the synchronizability of oscillator networks. We find that these topological factors produce marked signatures in the Laplacian eigenvalue distribution and in the localization properties of individual eigenvectors. Using a set of coordinates based on the Laplacian eigenvectors as a diagnostic tool for synchronization dynamics, we find that the process of frequency synchronization can be visualized as a series of quasi-independent transitions involving different normal modes. Particular features of the partially synchronized state can be understood in terms of the behavior of particular modes or groups of modes. For example, there are important partially synchronized states in which a set of low-lying modes remain unlocked while those in the main spectral peak are locked. We find therefore that spectra are correlated with dynamics in ways that go beyond results relating a single threshold to a single extremal eigenvalue.

DOI: 10.1103/PhysRevE.77.031102 PACS number(s): 89.75.Hc, 05.45.Xt

I. INTRODUCTION

In the recent intense activity that has focused on complex networks [1–4], one goal has been to identify properties of networks that are important for their function and behavior. A number of concepts have been introduced for classifying network structures, for example, degree distribution, path length [5], clustering [6], the small-world property [6,4], modularity, betweenness [7], etc. Diagnostic tools for assessing function include percolation properties, robustness against node or link deletion [8], studies of epidemic spreading [9], and various measures of synchronizabilty. Synchronization can be approached by means of global order parameters [10,11] or stability analyses of fully synchronized [12] or fully incoherent [11,13] states, which give thresholds for the onset of either synchronization or desynchronization.

One way of distilling information about a network is to analyze the eigenvalue and eigenvector spectra of matrices associated with the network, and that is the focus of this paper. Such spectral properties provide an important intermediary between structural and dynamical properties. They are derived directly from the network topology and many relations exist between particular eigenvalues and important network structural properties [14–16], while a number of studies have related extremal eigenvalues to dynamical properties and thresholds [12,13]. In the current paper we use spectral tools to diagnose the dynamics of partial synchronization, between the incoherent and fully coherent states.

The important matrices are derived from either the adjacency or coupling matrix. The adjacency matrix A_{ij} is defined by $A_{ij}=1$ if a connection exists between the nodes numbered i and j and $A_{ij}=0$ otherwise. The coupling matrix W_{ij} is simply the matrix of coupling strengths among nodes, and if the links are all equally weighted then it is a multiple of the adjacency matrix. Several definitions of the Laplacian matrix are in use. We will define it here as

$$L_{ij} = \left(\sum_j W_{ij} \right) \delta_{ij} - W_{ij}. \tag{1}$$

In the case where $W_{ij}=A_{ij}$, this matrix is sometimes known as the "combinatorial Laplacian." [17] The definitions and significance of these matrices will be discussed further in the following sections.

Some applications of network matrices depend only on one or two extremal eigenvalues. A widely known application of the Laplacian matrix is the master stability function (MSF) technique for analyzing the stability of a synchronized state of coupled oscillators [12]. For the MSF, the quantity of interest is the ratio of the largest to the smallest nonzero eigenvalue of the Laplacian, and accordingly many studies of the Laplacian spectrum on complex networks are limited to tabulations of this ratio. In mathematical graph theory, a number of theorems relate geometrical properties such as the diameter of the network to the smallest nonzero eigenvalue [15]. Likewise with the adjacency matrix, for some applications it is only the largest eigenvalue that matters. For example, under certain assumptions, approximate relations were derived between the largest eigenvalue of the adjacency matrix and the critical coupling strength for the onset of phase synchronization in a network of limit cycle oscillators [13].

In many cases, however, there is additional important information contained in the full spectrum and in the eigenvectors themselves. The Laplacian spectrum, for example, is relevant to the solution of diffusion and flow problems on networks [15]. Apart from the MSF formalism, it is applicable more generally to the dynamics of coupled oscillators near the synchronized state, including the relaxation of coupled identical limit-cycle oscillators to equilibrium [18]. In a previous paper [19], we showed that the eigenvectors of the Laplacian form a useful coordinate system in which to view the dynamics of partly synchronized networks of oscillators, even at a significant distance from full synchronization.

There have been relatively few efforts to study the full spectrum of the Laplacian as defined in Eq. (1) for general complex networks. In the mathematical literature, more attention has often been paid to the adjacency matrix [14] or the so-called "normalized Laplacian" [16,17] which is related to L but can have a quite different spectrum. Studies of the combinatorial Laplacian [15] are not often focused on applications to large complex networks. There have been some numerical and analytical studies of the adjacency matrices of complex networks [20,21,17,22] as well as some studies of the normalized Laplacian [17] and of the closely related "transition matrix" [22] on one category of random uncorrelated networks with given expected degree distributions. As for the Laplacian defined in Eq. (1), its full spectrum has been examined on random Erdos-Renyi [23] and small-world networks [24] but much of the territory is still relatively uncharted, especially in the case of networks with degree correlations, clustering, communities, and other types of correlations.

The current paper explores the information contained in the Laplacian spectrum, and the three-way linkage among network topology, spectrum, and dynamics, in particular oscillator synchronization dynamics. One goal is simply to characterize the Laplacian eigenvalues and eigenvectors for several important types of networks. We pay attention to the spectral and dynamical effects of network topological properties such as degree distribution (especially Poisson vs scale-free or homogeneous vs heterogeneous), clustering (i.e., the tendency of neighbors of a given node to form links with each other), and community structure, also known as modularity. While recent studies of network matrix spectra have dealt with random network models without correlations, modularity and clustering represent significant new ingredients. In addition, we consider weighting and symmetry or asymmetry of connection strengths, especially the asymmetric connection scheme in which the total input to each node is normalized. We are interested in the latter coupling scheme because it is known to optimize synchronizability in MSF terms [25,26].

Beyond the mere classification of spectra, another goal is to understand dynamics. For the types of networks studied, we consider the synchronization dynamics of coupled phase oscillators (the Kuramoto [11] model), using coordinates based on the Laplacian eigenbasis as a tool for visualizing the dynamics and revealing structure within the synchronization transition. This program follows the general inspiration of the MSF technique in that the aim is to use the Laplacian spectrum to isolate topological influences on synchronization, as distinct from the individual node dynamics. The MSF, however, is strictly applicable only to the stability problem of a fully synchronized state of a set of exactly identical oscillators. It is most useful for networks of identical chaotic oscillators. For appropriately limited questions, the MSF, relying only the eigenratio, gives rigorous answers. The present work, on the other hand, seeks rather more heuristic tools for much broader questions. We consider nonidentical oscillators and we consider the process of synchronization from its onset up to nearly complete synchronization, rather than being limited to the immediate neighborhood of the synchronization manifold. The current paper follows a Brief Report [19] in which a subset of our results was presented. We expand on those results here by studying a greater variety and larger sample of networks and by examining properties of the individual eigenvectors such as localization and degree bias.

The remainder of the paper is organized as follows. Section II discusses some general properties of the Laplacian matrix that are relevant to network dynamics. Section III is devoted to a description of particular network Laplacian eigenvalue spectra and their dependence on topological properties. In Sec. IV we then consider some properties of the eigenvectors themselves, especially localization and degree bias. Finally, in Sec. V, we examine some connections between spectra and dynamics in the case of a network version of the Kuramoto model. A coordinate system for phase space based on the Laplacian eigenvectors proves useful for obtaining a geometric picture of the oscillators' dynamical behavior. Under some conditions, groups of eigenvectors behave as dynamically independent degrees of freedom and the process of synchronization amounts to a contraction of phase space onto progressively lower-dimensional submanifolds spanned by lower-eigenvalue eigenvectors. The concluding Sec. VI summarizes our results and suggests some future directions.

II. PROPERTIES AND SIGNIFICANCE OF THE LAPLACIAN

We begin by reviewing and extending some known general properties of the Laplacian of a network of N nodes. We denote the N-component eigenvectors and associated eigenvalues, respectively, by $\mathbf{V}^\alpha$ and λ_α, so that

$$\sum_{j=1}^{N} L_{ij} V_j^\alpha = \lambda_\alpha V_i^\alpha. \tag{2}$$

From the definition (1) it follows that the sum of matrix elements in any row is zero, and consequently the constant vector $(1,1,\ldots,1)$ is always an eigenvector with eigenvalue zero. If the coupling matrix is symmetric ($W_{ij}=W_{ji}$) then so is the Laplacian, and therefore all eigenvalues are real and eigenvectors corresponding to different eigenvalues are orthogonal. The trace of L is given by

$$\mathrm{Tr}\, L = \sum_i L_{ii} = \sum_j \sum_i W_{ij} - \sum_i W_{ii}. \tag{3}$$

(From now on, limits of summations are suppressed and assumed to be from 1 to N unless otherwise indicated.) If self-couplings are excluded, then the final term vanishes as $W_{ii}=0$. If, furthermore, $W_{ij}=A_{ij}$ (i.e., all couplings equally weighted) then the row sum of W is just the degree (or number of neighbors) of each node, and so

$$\sum_\alpha \lambda_\alpha = \mathrm{Tr}\, L = \sum_i k_i, \tag{4}$$

where $k_i=\Sigma_j W_{ij}$ is the degree of the ith node. Some authors (e.g., [15]) define the quantity $\Sigma_j W_{ij}$ as the "degree" even when the couplings W_{ij} are not only zeros and ones. However, it is useful to be able to distinguish the sum of cou-

plings from the actual number of nodes to which a given node is connected. In cases of possible confusion, we suggest the term "topological degree" for the latter, and following the nomenclature of Ref. [26], we use "intensity" to refer to the sum of input coupling strengths. For general couplings, Eq. (4) remains valid if the degree is replaced by the intensity. This means that the average of the Laplacian eigenvalues is equal to the average degree (or intensity) $\langle k \rangle$ for the whole network, and consequently $\langle k \rangle$ is a convenient scaling factor for comparing spectra of different networks [40].

A useful identity is the following:

$$\sum_{i,j} L_{ij} x_i x_j = \sum_{i,j} W_{ij} (x_i - x_j)^2, \tag{5}$$

where x_i may be any quantity associated with each node (in the context of synchronization, it could be the phase of each oscillator). The above guarantees that, as long as the couplings are non-negative, then the Laplacian is positive semidefinite; i.e., all of its eigenvalues are positive or zero. If x_i represents a perturbation of some dynamical degree of freedom (such as the phase of an oscillator) then Eq. (5) suggests a heuristic interpretation of L as a tensor expressing the rigidity of the network against such perturbations. In particular, if the perturbation is a multiple of one of the normalized eigenvectors, or in other words if

$$x_i = \eta V_i^{\alpha},$$

then

$$\sum_{i,j} W_{ij} (x_i - x_j)^2 = \lambda_{\alpha} \eta^2. \tag{6}$$

The left-hand side of Eq. (6) is a sum of squared differences across links, weighted by the strength of each link; it can be imagined as a sum of potential energies due to stretched bonds. If the eigenvalue λ_{α} is small, then the perturbation along the corresponding vector can occur without disturbing very many strong bonds, and the opposite is true if λ_{α} is large. With this interpretation in mind, the zero mode $(1,1,\ldots,1)$ indicates the freedom of a uniform translation of the whole network (in the case of coupled oscillators, it is the freedom to reset all phases by an equal amount without affecting any links).

The definition (1) shows a deceptively simple relationship between the adjacency (or coupling) matrix and the Laplacian. However, it is only in the special case of a so-called *regular network* (i.e., one in which the degree or the sum $K = \Sigma_j W_{ij}$ is the same for all i) that the two matrices commute and thus are guaranteed to share a common eigenbasis. In this special case, the corresponding eigenvalues λ_{α} for the Laplacian and μ_{α} for the coupling matrix are related by $\lambda_{\alpha} = \mu_{\alpha} - K$. In general, it is easy to show that the commutator

$$[\mathbf{W},\mathbf{L}] \equiv \mathbf{WL} - \mathbf{LW} \tag{7}$$

is a matrix whose elements are proportional to the differences between the degrees of adjacent nodes. This leads us to expect that the differences in spectrum between the two matrices become more important as the network becomes more heterogeneous, but on the other hand can be lessened by what is called assortative mixing [27] (i.e., a tendency of nodes to connect with other nodes of similar degree).

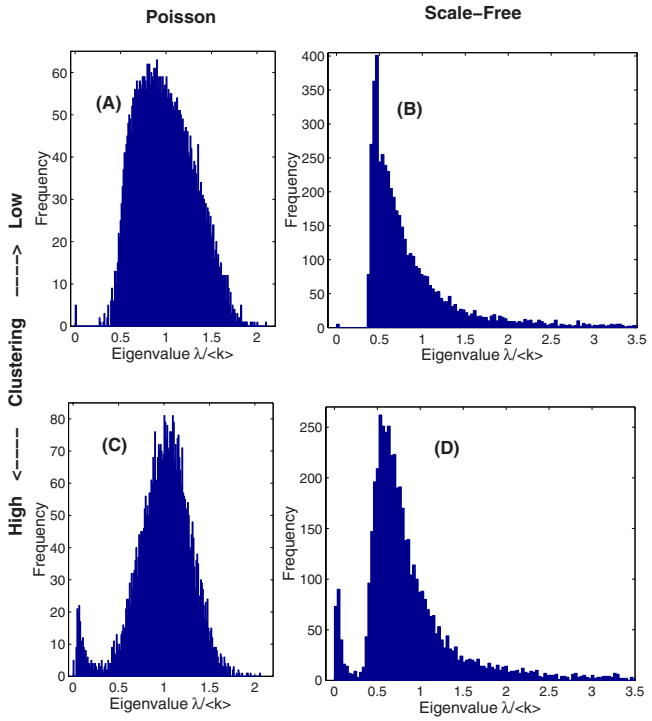

FIG. 1. (Color online) Histograms of scaled Laplacian eigenvalues for Poisson and scale-free networks with low and high clustering coefficients. Each histogram is cumulative for five different networks drawn from the same ensemble. Note that the tails have been truncated for the scale-free networks—they extend to $\lambda/\langle k \rangle \approx 10$ and are shown in Fig. 2 on a logarithmic scale.

III. TOPOLOGY AND LAPLACIAN SPECTRA

In this section we examine the shapes of the Laplacian spectra of several types of networks and consider how specific features of the spectra are correlated with structural features of the networks. We will begin with networks in which all existing links are bidirectional and equally weighted, and then consider certain types of asymmetries. Except where otherwise indicated, the networks we study have $N=1000$ nodes and average topological degree $\langle k \rangle = 20$. Figures 1(a) and 1(b) show histograms of the (scaled) Laplacian eigenvalue distributions for random (Erdos-Renyi [28]) networks with Poisson degree distribution [henceforth referred to as a Poisson network (PN)] and Barabasi-Albert [29] networks with scale-free distribution [a scale-free network (SFN)]. The first thing to note is the dependence of the spectrum on the degree distribution. The eigenvalue distributions share some statistical features of the degree distributions: for example, the eigenvalue spectrum of the SFN has a power-law tail just as does the degree distribution. For the Poisson networks, on the other hand, the spectrum has a Poisson-like single peak with no significant tail. When we varied $\langle k \rangle$ from 5 to 40 (plots are not shown here), we found that the relative width

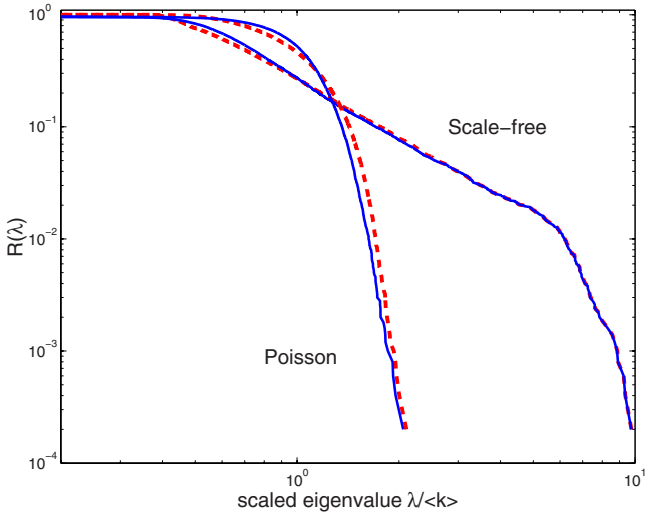

FIG. 2. (Color online) Integrated eigenvalue distributions $R(\lambda) \equiv \int_{\lambda}^{\infty} P(\lambda')d\lambda'$ for scale-free and Poisson networks with low (dotted line, red online) and high (solid line, blue online) clustering coefficient. The distributions for the SFNs follow a power law (straight line on the logarithmic scale) over a broad range of eigenvalues.

(or width scaled by $\langle k \rangle$) of this peak decreases with increasing $\langle k \rangle$ but that other qualitative features are the same.

In order to study the tails of the distributions more clearly, we plotted cumulative (integrated) eigenvalue distributions $R(\lambda) \equiv \int_{\lambda}^{\infty} p(\lambda')d\lambda'$, where $p(\lambda)$ is the differential eigenvalue density, on a log-log scale in Fig. 2. (The integrated distribution is useful for numerically studying tails because it avoids some of the problems associated with histogram bins in the differential distribution having either no points or small numbers of points.) The SFN shows significant finite-size effects in both the high and low-eigenvalue cutoffs, but there is a region of the distribution that clearly obeys a power law (a straight line on the logarithmic plot). For the low-clustering SFN, the best-fit slope of the cumulative plot within the range $0.5 < \lambda_i < 5$ is -1.73, corresponding to an exponent for the eigenvalue distribution of -2.73. (Note that the finite-size BA network does not give a power-law exponent of exactly 3 as one expects in the large-N limit: empirically, the degree distributions for our SFNs have an exponent of -2.76.) Note that the increase in clustering has very little effect on the outer tail of the eigenvalue distribution, although, as we will see later, it does affect properties of the eigenvectors themselves. For comparison, we also generated networks with scale-free distributions of expected degrees with exponents 2.5, 3.0, and 3.5 according to the model described in Refs. [17,30]. We found that in all cases the tails of the eigenvalue distributions follow power laws with the same exponents (or within 1% to 2%) as the degree distributions. The power-law dependence in the cases of the "expected degree" networks is in fact cleaner than for the BA model, lacking the knee at large eigenvalues that is visible in Fig. 2.

We next examine the effect of clustering, which is known to have strong effects on the synchronizability of networks [31]. We applied a stochastic rewiring algorithm [32,31] to increase the clustering coefficient of the PN and SFN while leaving the degree distributions unchanged. Clustering (also called transitivity) refers to the tendency of two nodes which share a common neighbor to have an increased likelihood of also being directly connected to each other (compared to two nodes that do not share a neighbor) [6]. Put another way, clustering indicates the prevalence of triangles in the network topology. The clustering coefficient γ, a numerical measure of clustering, is defined as an average over the network of the local clustering coefficient, given by

$$\gamma_i = \frac{t_i}{\binom{k_i}{2}} = \frac{2t_i}{k_i(k_i-1)}, \tag{8}$$

where t_i is the number of mutual connections among the neighbors of a given node, k_i is the number of neighbors, and $\binom{k_i}{2}$ is the number of possible pairs of neighbors that could potentially be connected. The bottom row of plots in Fig. 1 show the spectra of networks with the same degree distributions as the ones above, but with high clustering coefficients, specifically $\gamma = 0.640 \pm 0.005$ for the PNs and $\gamma = 0.675 \pm 0.005$ for the SFNs. For the "natural" low-clustering networks whose spectra are in the upper row of Fig. 1, the values are within the range $\gamma = 0.0195 \pm 0.0005$ for the PNs and $\gamma = 0.073 \pm 0.005$ for the SFNs. It is apparent that for both the PN and SFN, increasing the clustering changes the shape of the main spectrum slightly, sharpening the peak and shifting it to the right, while also creating a new group of eigenvalues close to zero. A series of plots at intermediate values of γ (not given here) shows that as γ increases, this group of eigenvalues breaks away from the main peak and gradually migrates downward toward zero.

The presence of near-zero eigenvalues generally indicates the existence of strong communities, or nearly disconnected components. The multiplicity of the (exactly) zero eigenvalue is equal to the number of disconnected components [15]. Strong communities (subsets of nodes with much fewer connections between groups than within groups) behave like nearly disconnected components and thus result in small but nonzero eigenvalues. Low eigenvalues and the corresponding eigenvectors have been used in some algorithms for partitioning and/or detection of communities [33–35]. The essential technique is as follows: the m eigenvectors with the lowest nonzero eigenvalues are found, and each node is assigned m coordinates which are the entries of the m eigenvectors at the position of that node. When these coordinates are plotted for all nodes, communities, if they exist, appear as groups of nodes clumped together in this m-dimensional space [34,35]. We have made such a plot for the first three eigenvectors of the high- and low-clustering SFNs in Fig. 3. The plot clearly shows that the nodes of the high-clustering network group together into communities while those of the low-clustering network do not. In examining synchronization dynamics in Sec. V, the low-lying eigenvectors will give a good indication of the dynamical importance of communities. In view of the interpretation of L as giving the network's inherent rigidity against perturbations, the low-lying eigen-

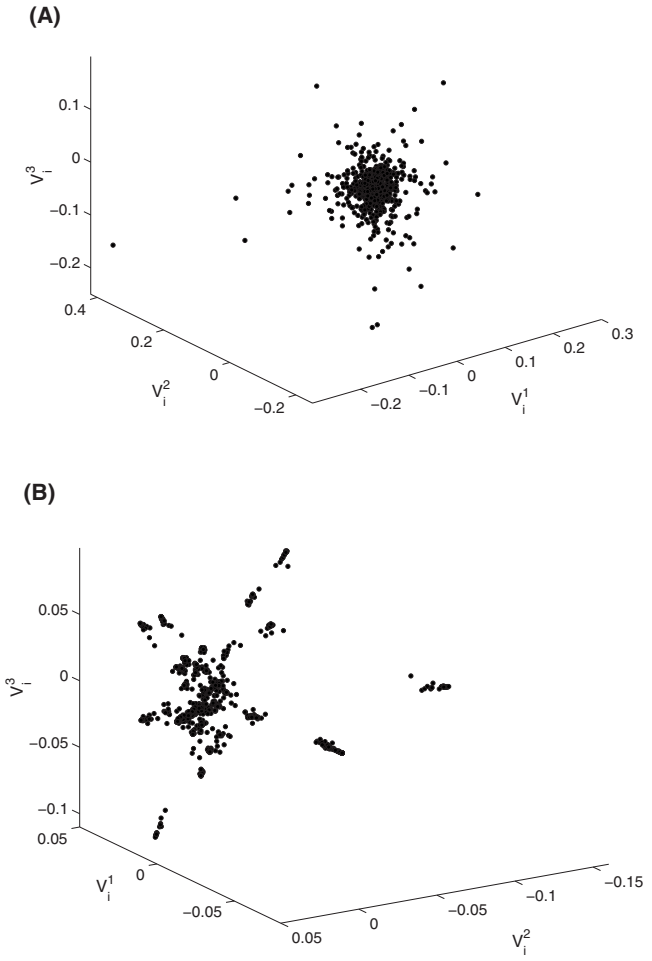

FIG. 3. Scatter plots of the components of the Laplacian eigenvectors with the lowest three nonzero eigenvalues for scale-free networks with low (top) and high (bottom) clustering. In the high-clustering case, communities appear as clumps of nodes.

vectors associated with communities reflect the relative ease with which the network can fall apart (or desynchronize) along community boundaries.

Although in network studies it it most common to consider networks with symmetric, undirected links, Motter *et al.* [25,26] have shown for a variety of topologies that the MSF synchronizability as measured by the eigenratio λ_N/λ_2 is improved by a particular scheme of asymmetric coupling which we refer to here as input normalization or simply *normalization*. This is a weighting in which the input coupling strengths to any node are scaled so that their sum is unity. Put another way, the coupling matrix is derived by dividing each row of the adjacency matrix by the degree of the corresponding node:

$$W_{ij} = A_{ij}/k_i = \frac{A_{ij}}{\sum_j A_{ij}}. \tag{9}$$

In a heterogeneous network, this implies that the couplings are not symmetric. If a hub node H with high degree is connected to a peripheral node P with low degree, then the influence of H on P is greater in absolute terms than that of P on H. P's influence on H is diluted by H's many other neighbors. Motivated by the enhanced synchronizability of normalized networks, we are interested in understanding the effect of normalization on the full Laplacian spectrum (and subsequently on dynamics), not only the extremal eigenvalues. In spite of the asymmetry introduced into the coupling and therefore the Laplacian, it can be proved [25] that the Laplacian eigenvalues are still all real in this case. Furthermore, the intensities of all nodes are unity, so that, as discussed above, the Laplacian has a common eigenbasis with the coupling matrix. (Due to the asymmetry, however, the eigenvectors are not mutually orthogonal.) The eigenvalue spectrum is in fact the same as for what is known in graph theory as the "normalized Laplacian," [16,17] of the underlying unweighted network, although the eigenvectors themselves are not the same. To summarize the relationships among the matrices, let $\mathbf{D}$ be the diagonal matrix whose entries are the topological degrees, let $\mathbf{L}_u$ and $\mathbf{L}_n$ be the Laplacians of the unnormalized and normalized networks, repectively, while $\mathcal{L}$ is the symmetric "normalized Laplacian." Then the relationships are

$$\mathbf{L}_u = \mathbf{D} - \mathbf{A},$$

$$\mathbf{L}_n = \mathbf{L}_u \mathbf{D}^{-1},$$

$$\mathcal{L} = \mathbf{D}^{-1/2} \mathbf{L}_u \mathbf{D}^{-1/2}. \tag{10}$$

Figure 4 shows eigenvalue histograms for the same networks as in Fig. 1, but with the inputs normalized. The first striking feature is that the spectra look very nearly the same for both the PN and the SFN. As was found in [26], the effect of degree heterogeneity is greatly suppressed by normalization; we will see that this is also true of the effect of degree distribution on dynamics. In the low clustering case, the spectra have approximately semicircular shapes for both networks, recalling the so-called semicircle law [36,37] for spectra of random matrices. Previously, the normalized Laplacians of a broad class of uncorrelated random matrices (including the Erdos-Renyi but not, strictly speaking, the Barabasi-Albert network) were found to obey the semicircle law [17], as were the closely related transition matrices [22]. Consistent with what is known about the eigenratio [25], the spectra are much narrower than for the unnormalized networks, with no apparent tail either of the exponential or power-law type.

Increasing the clustering of the normalized networks narrows and markedly sharpens the main spectral peak into a more triangular shape. The other main effect of clustering, namely the creation of a second peak near zero, is much the same as in the unnormalized networks. This is consistent with our understanding of the low modes as being associated with community structure. Communities are a topological phenomenon, the result of a paucity of connections among the different subsets. If there are only a few connections between two subsets of the network, then an adjustment of coupling *strengths* alone is unlikely to compensate significantly for this scarcity, unless some bias results in extra strengthening of intercommunity ties at the expense of oth-

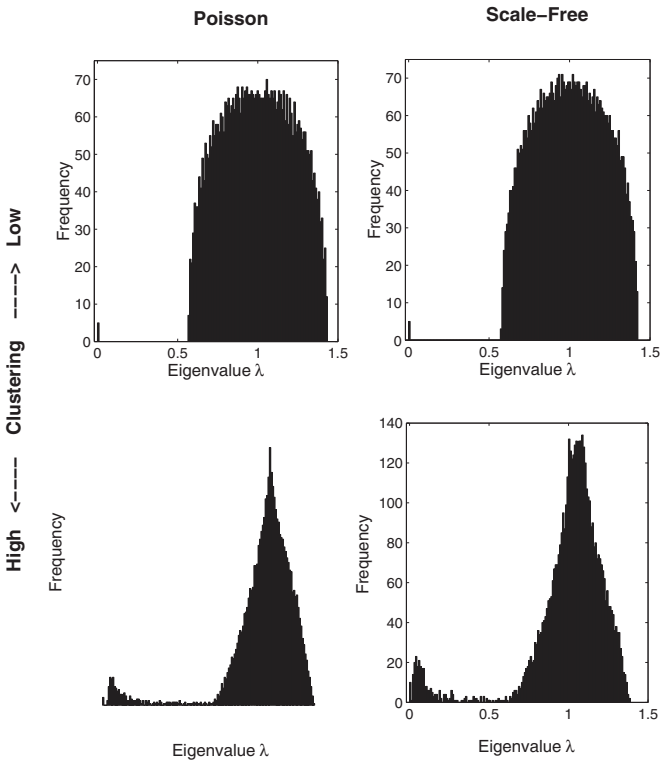

FIG. 4. Eigenvalue histograms for networks with normalized inputs [Eq. (9)]. The networks are topologically the same as in Fig. 1; only the connections strengths have been changed. Since all nodes have a coupling sum of unity, the scaling factor $\langle k \rangle$ is not needed here: the eigenvalues λ in Figs. 4, 8, and 9 are comparable to the scaled values $\lambda/\langle k \rangle$ in Figs. 1, 6, and 7.

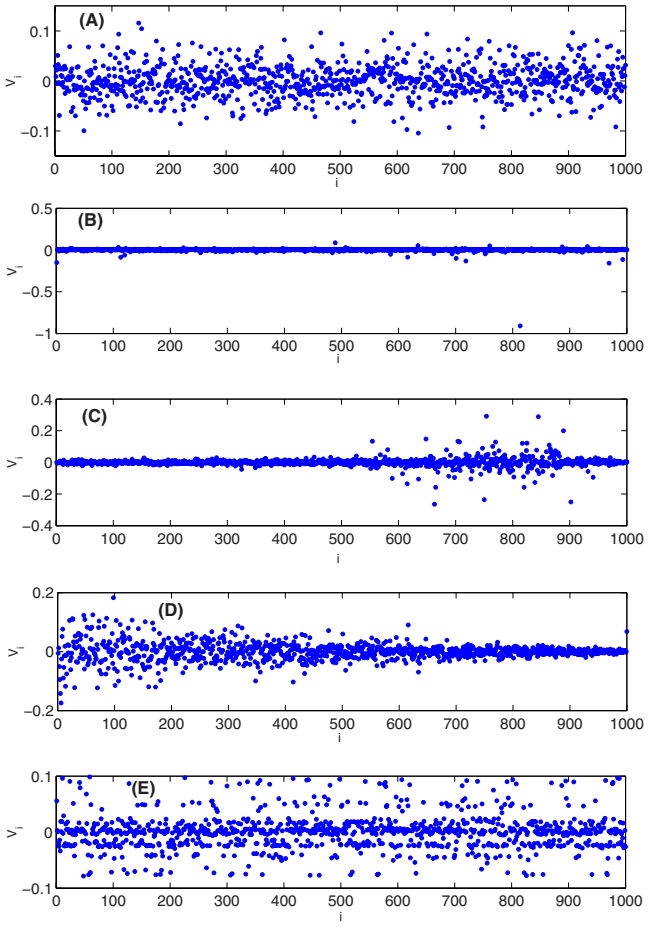

FIG. 5. (Color online) Examples of different shapes of Laplacian eigenvectors. Each is typical for one type of network and a particular range of eigenvalues. x coordinates are the node index, where the nodes have been sorted from lowest to highest degree; y coordinates are the eigenvector components. (a) Low-clustering PN, vector $\alpha=500$ (i.e., the vector with the 500th lowest eigenvalue), $\lambda=19.27$. This vector is delocalized and its components appear random. (b) Low-clustering PN, $\alpha=4$, $\lambda=7.97$. This vector is strongly localized: note the single large component at $i\approx 810$. (c) Low-clustering SFN, $\alpha=800$, $\lambda=23.74$. Not strongly localized, but most large components occur at nodes within a medium to high range of degrees. (d) Low-clustering SFN, $\alpha=50$, $\lambda=8.26$. Largest components occur at low-degree nodes. (e) High-clustering PN, $\alpha=4$, $\lambda=0.86$. This is an example of the low-lying modes that form in networks with high clustering. Components fall near a small number of discrete values, giving the plot a striated appearance.

ers. Input normalization certainly alters the dynamical roles of high- vs low-degree nodes, but it is not surprising that it has little effect on such global topological features as community formation.

IV. SHAPES OF THE EIGENVECTORS: LOCALIZATION AND DELOCALIZATION

To the extent that different Laplacian eigenvectors are associated with collective degrees of freedom having different dynamical functions, it is interesting to examine the "shapes" of these vectors and understand how they relate to the network's structure. In Fig. 5, we plot the components V_i^α of several representative eigenvectors against the node index i where the nodes have been sorted from lowest to highest degree. While all plots appear partly random, reflecting the randomness in the network's structure, there are nonetheless patterns that are clear from a visual inspection, and clear qualitative differences between different vectors. Some vectors, such as the one shown in Fig. 5(b), are highly localized, with only a few large nonzero components and the rest nearly zero, while others such as the one in Fig. 5(a) have nonzero components spread throughout the whole network. Some, such as Fig. 5(c) or 5(d), show a degree bias; most of their large components occur at nodes within a certain degree range (either high, low, or intermediate). The vector in Fig. 5(e) is an example of one of the low-lying modes in a strongly clustered network. The components cluster around a small number of discrete values. Nodes having the same value of V_i are likely to belong to the same community. (As described above, the communities are separated more distinctly if several low-lying eigenvectors are plotted simultaneously.)

A convenient scalar measure of a vector's degree of localization is the so-called inverse participation ratio [11] (IPR) P, which is defined for any vector $\mathbf{V}$ by

$$P(\mathbf{V}) = \frac{\sum_i V_i^4}{\left(\sum_i V_i^2\right)^2}. \tag{11}$$

(Note that the denominator is 1 if the vector is normalized.) P ranges from a minimum value of $1/N$ (for a normalized vector whose components are all of equal magnitude $1/\sqrt{N}$) to a maximum of 1 for a vector with only one nonzero component. The more localized the vector (i.e., the less evenly its weight is spread among multiple components) the higher the value of P. In order to quantify the degree bias noted for some of the eigenvectors, let us define the degree expectation value (DEV) Q for a vector as

$$Q(\mathbf{V}) = \frac{\sum_i V_i^2 k_i}{\sum_i V_i^2}. \tag{12}$$

[Some other authors [23] have used instead the "center connectivity," which is simply the degree of the node with the maximum value of $|V_i|$. The center connectivity should be nearly identical to the DEV in cases of vectors localized very strongly at a single node, but Q, being an average, is likely to be a more robust and meaningful metric in cases such as Fig. 5(c) where a vector has some level of localization and degree bias but no single component is dominant.]

Figures 6–9 show values of P and $Q/\langle k\rangle$ (i.e., the DEV scaled by the average degree) for the Laplacian eigenvectors of several networks, plotted against the corresponding scaled eigenvalues $\lambda/\langle K\rangle$. (Note that while Q is appropriately scaled by the average topological degree, the eigenvalues are scaled by the average intensity, which is equal to the topological degree for the unnormalized networks but unity for the normalized ones.) In the plots for the unnormalized networks (Figs. 6 and 7), several features are notable. Among modes within the main spectral peak, those near the edges tend to be more strongly localized. For both Poisson and scale-free networks, increased clustering tends to increase the localization of modes, especially in the tails of the eigenvalue distributions. The DEVs are positively correlated with the eigenvalues, especially in the scale-free case and for the tails of the eigenvalue distributions. An exception to these trends is the group of low-lying modes that form at high clustering. These modes are generally rather delocalized and have Q close to the average degree of the network. This is consistent with their interpretation as reflecting global community divisions of the network, involving most of the nodes. We note that our results for the spectra, IPRs, and DEVs for the low clustering Poisson networks agree with random network results reported elsewhere [23]. The other results are largely consistent with the general principle that localization tends to occur near "defects" or nodes with degrees significantly higher or lower than average [23]. A notable exception occurs for the strongly clustered SFN, where there is a large group of moderately to strongly localized modes with scaled eigenvalues near unity (see Fig. 6). From Fig. 7 it is evident that the DEVs of these modes fall near the average of the degree distribution, not the tails.

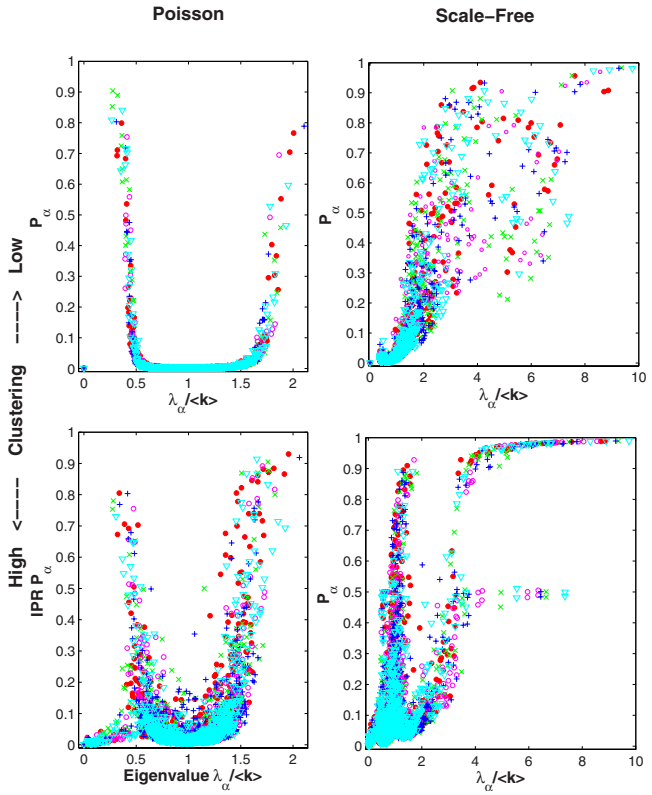

FIG. 6. (Color online) Inverse participation ratios P_α [Eq. (11)] of Laplacian eigenvectors for unnormalized networks, plotted against the corresponding scaled eigenvalues. Here and in all of Figs. 6–9, different symbols (colors) are for five different networks from the same ensemble.

Analogous plots of eigenvector properties for normalized networks (Figs. 8 and 9) show radical differences from the unnormalized case. First, there is much less localization of modes, even at high clustering. The dependence of DEV on eigenvalue is much weaker and not monotonic. Rather, the main peak of the spectrum is approximately symmetric about $\lambda=1$. In the normalized network unlike the unnormalized case, the Laplacian spectrum is directly related to that of the coupling matrix, and a Laplacian eigenvalue of 1 corresponds to a coupling matrix eigenvalue of 0. It is a general property of random graphs that their adjacency matrix spectra are approximately symmetric about zero (deviations from symmetry occur when there are correlations or clustering) [20]. The spectra of normalized networks evidently share this approximate symmetry, although the coupling matrix in this case is *not* the same as the adjacency matrix. It should be kept in mind that the eigenvectors of L for a normalized network are not orthonormal. In contrast to the main peak, the low-lying modes of strongly clustered networks behave qualitatively much like those in unnormalized networks, suggesting again that community structure is scarcely affected by normalization.

Without making a thorough analysis of the dependence of spectra on $\langle k\rangle$ or the finite size N, we confirmed that plots of the eigenvalue distributions, IPRs, and DEVs (not shown here) for scale-free and Poisson networks with $N=1500$ and

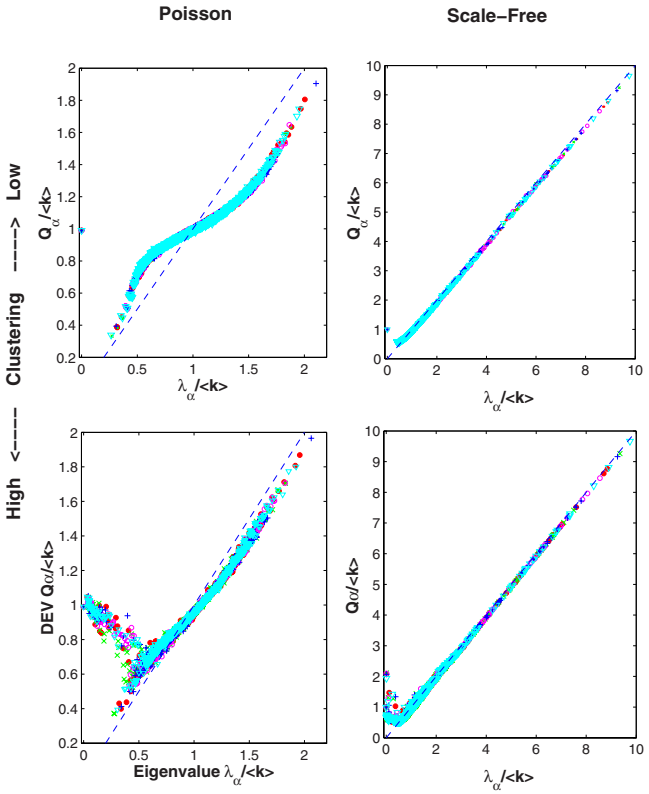

FIG. 7. (Color online) Scaled degree expectation values $Q_\alpha/\langle k\rangle$ [Eq. (12)] for Laplacian eigenvectors of unnormalized networks. Eigenvalues and DEVs are strongly correlated in all cases (a dotted line with slope 1 is shown for comparison).

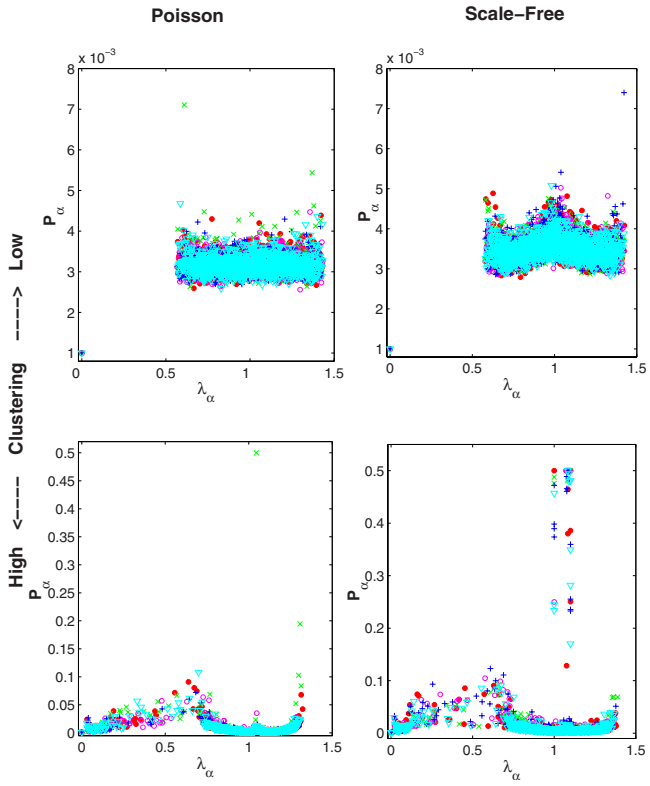

FIG. 8. (Color online) Inverse participation ratios P_α of Laplacian eigenvectors for normalized networks.

$\langle k\rangle=10$ show very much the same features as in the $N=1000$, $\langle k\rangle=20$ case, including the same changes with increased clustering coefficient, provided that the eigenvalues are always scaled correspondingly by $\langle k\rangle$. One difference is that the relative width of the Poisson distribution decreases with increasing $\langle k\rangle$.

V. SPECTRA, EIGENCOORDINATES, AND DYNAMICS

In this section, we examine numerically the synchronization behavior of a network Kuramoto [11] model on the networks we have been studying. Topological features (degree distribution, clustering, normalization) have strong and sometimes complex effects on synchronization [31,25,26,12]. We show that projections onto the Laplacian eigenbasis are useful in understanding these effects, and that specific dynamical behaviors of the networks are associated with specific sets of modes in the Laplacian spectrum. This is true even in strongly nonlinear regimes of partial synchronization, despite the fact that the Laplacian is most naturally applied to linear problems near full synchronization.

We first define the model and show how the Laplacian and its spectrum appear naturally in a linearized description of the frequency-synchronized state, and then we proceed to use the Laplacian eigenvectors to parametrize the partially desynchronized states, showing that this coordinate system remains useful well beyond the range of validity of the linearization and that individual modes may behave as quasi-independent degreess of freedom.

Our model [38] is defined by the coupled equations

$$\frac{d\phi_i}{dt} = \omega_i + \frac{\beta}{\langle K\rangle}\sum_j W_{ij}\sin(\phi_i - \phi_j), \tag{13}$$

where ϕ_i are N phase variables (one associated with each node of a network), $-1\le\omega_i\le 1$ are the randomly and uniformly distributed intrinsic frequencies, β is the overall coupling strength, and W_{ij} as before is the weighting matrix of the individual couplings. The coupling strength is scaled by the average intensity $\langle K\rangle$ of all nodes. In our simulations, we imposed the condition $\bar{\omega}=0$ by subtracting the average from each realization of the random frequencies. (This condition can be imposed without loss of generality; it amounts to a transformation to a rotating frame of reference.) If the couplings are symmetric, then the velocities $\frac{d\phi_i}{dt}$ obey the exact sum rule

$$\sum_i \frac{d\phi_i}{dt} = \sum_i \omega_i = 0 \tag{14}$$

due to the antisymmetry of the sine coupling function: when summed over i, the coupling terms in Eq. (13) cancel. Note that Eq. (14) does not necessarily hold for a normalized network, due to the asymmetry of the coupling W_{ij}.

If the system is strongly synchronized so that all phase differences are small, then the sine function can be linearized and the equations of motion become approximately

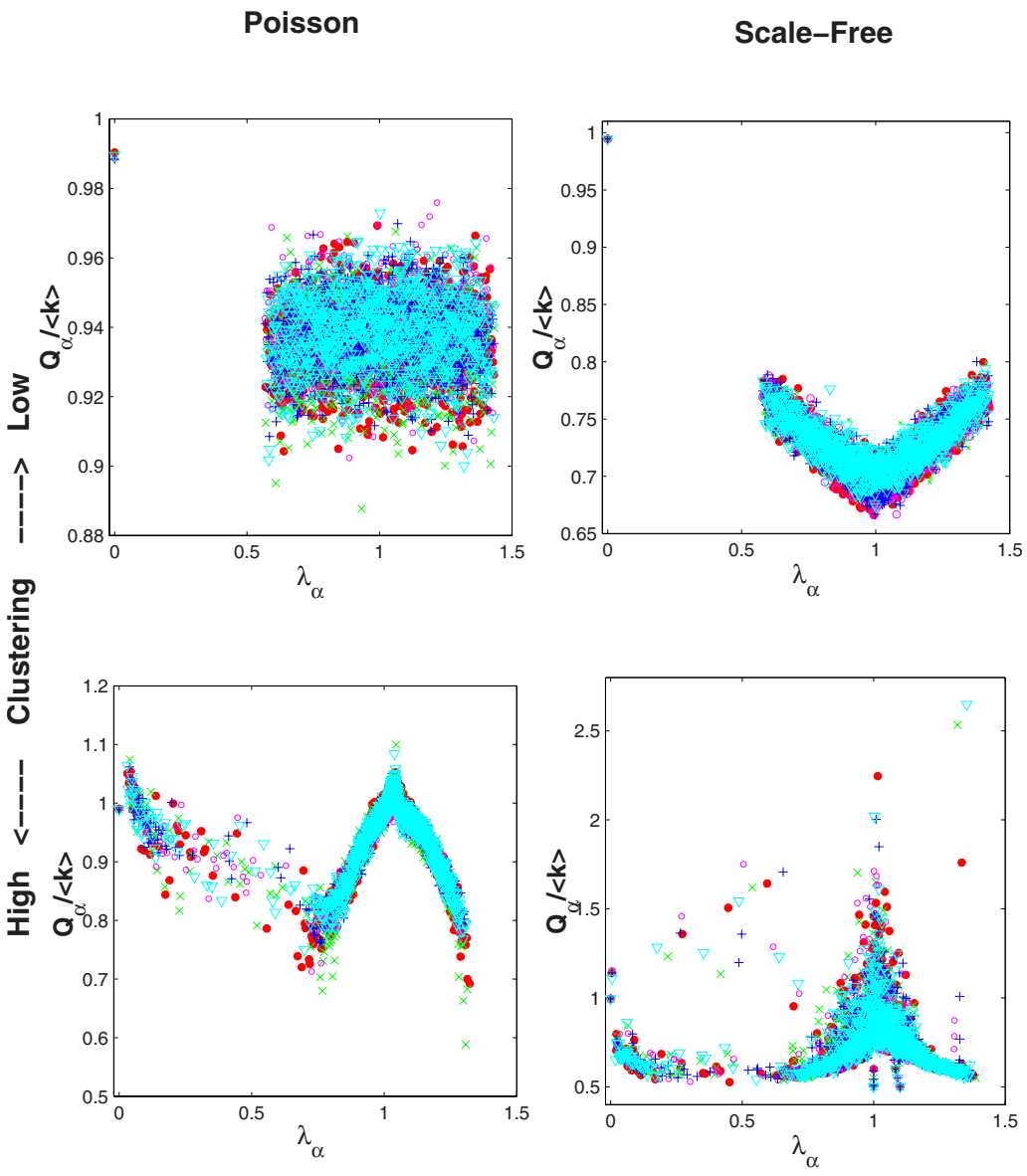

FIG. 9. (Color online) Degree expectation values Q_α for Laplacian eigenvectors of normalized networks.

$$\frac{d\phi_i}{dt} = \omega_i + \frac{\beta}{\langle K\rangle}\sum_j W_{ij}(\phi_i - \phi_j) = \omega_i - \frac{\beta}{\langle K\rangle}\sum_j \pounds_{ij}\phi_j. \tag{15}$$

Thus the Laplacian matrix appears naturally in the description of small deviations from full synchronization.

We simulated the model (13) using a fourth-order Runge-Kutta method with time step 0.1. In Fig. 10 we show the global synchronization order parameter

$$r = \left\langle \left| \sum_j e^{i\phi_j} \right| \right\rangle_T \tag{16}$$

(where $\langle\ \rangle_T$ signifies a time average) as a function of the coupling strength β for all of the network types considered in the previous sections. In the simulations, the time average was approximated by sampling 30 times at intervals of ten time units, after first running for 200 time units in order to reach a steady state. The results were then averaged over ten realizations of the random frequency distribution for each of five networks drawn from the ensemble. Note that in all cases, increasing the clustering strongly suppresses full synchronization, as shown by the fact that the order parameter curves for the highly clustered networks approach unity much more slowly at large coupling strength. This effect is more pronounced for the SFN than for the PN, whether normalized or not. For the unnormalized SFN, however, increased clustering has the seemingly contradictory effect of promoting the onset of partial synchronization even though it inhibits full synchronization. This effect, noted previously in [31] and confirmed by finite size scaling analysis [39] is apparent in the early upward turn in the order parameter curve at $\beta \approx 0.5$. It was found previously that it is the highest-degree nodes which synchronize first. This advanced partial synchronization disappears, however, in the case of

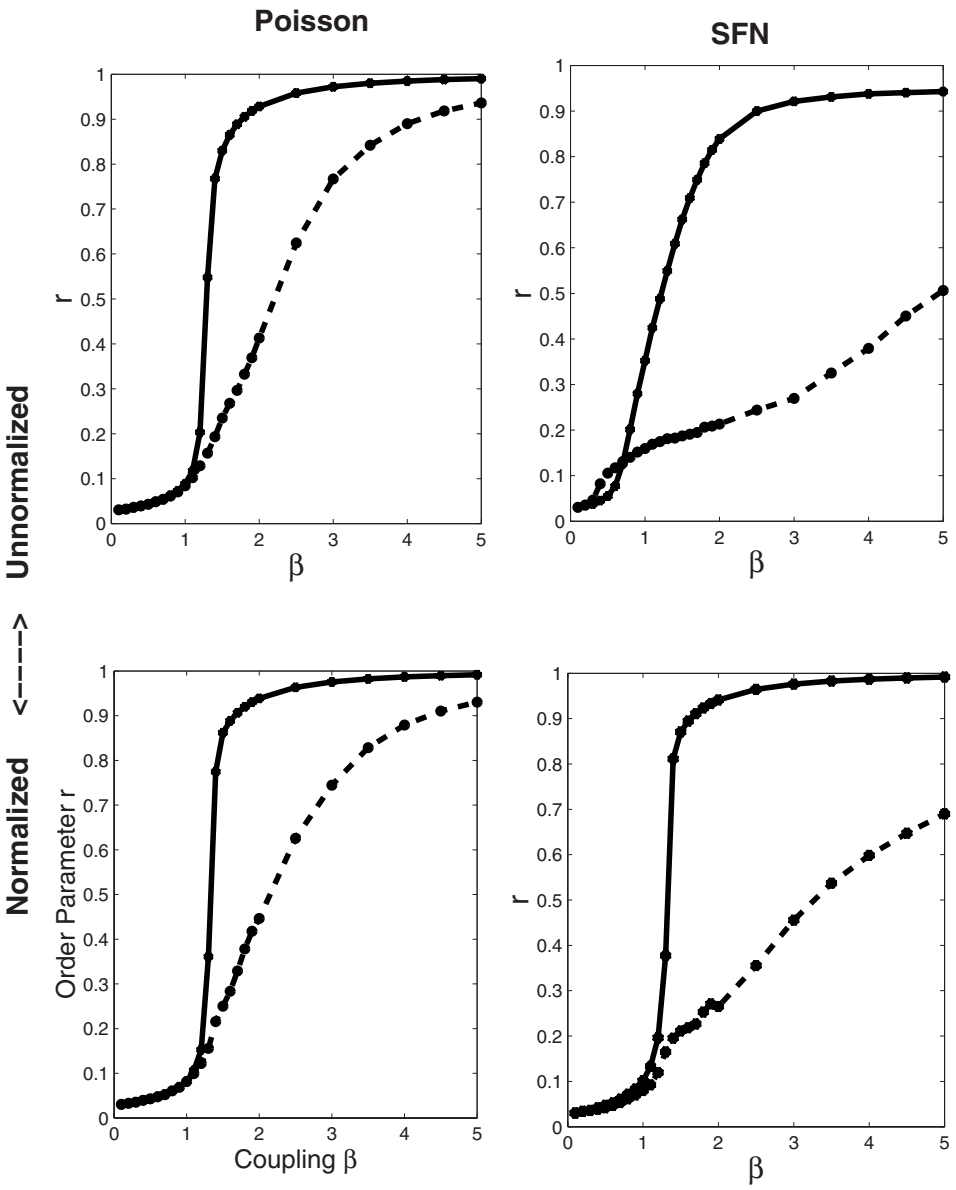

FIG. 10. Global order parameter vs coupling strength for Poisson and scale-free networks with low and high clustering. Solid line: low clustering and dashed line: high clustering. For the unweighted SFNs, note that there is a range of low couplings $0.3 \lesssim \beta \lesssim 0.7$ for which the highly clustered network is more synchronized than the low-clustering one.

normalized inputs. Since the advanced synchronization is associated with a special behavior of the high-degree nodes, its disappearance is consistent with the general observation that input normalization greatly reduces the effects of degree heterogeneity.

In [31] it was shown that nodes in different parts of the degree distribution can play different dynamical roles: for example, in the case of the SFN it is the hubs (high-degree nodes) that synchronize first. A complementary way of viewing the synchronization dynamics is to examine it in terms of appropriately chosen collective degrees of freedom rather than the behavior of individual oscillators. Here as in [19], we define collective coordinates by means of projections onto eigenvectors of the Laplacian. We define projections of the phase and frequency vectors onto these eigenvectors by

$$\phi^\alpha \equiv \sum_i \phi_i V_i^\alpha, \quad \omega^\alpha \equiv \sum_i \omega_i V_i^\alpha. \tag{17}$$

The *normal coordinates* ϕ^α are the appropriate ones for describing the relaxation to equilibrium of a strongly synchronized system [31,18]. In addition, we define the observed frequencies (rotation numbers) of the oscillators as the time averages

$$\Omega_j = \left\langle \frac{d\varphi_j}{dt} \right\rangle_T. \tag{18}$$

Projecting the vector of observed frequencies onto the Laplacian eigenbasis gives a time-averaged velocity along the direction defined by each eigenvector:

$$\Omega^\alpha = \sum_j \Omega_j V_j^\alpha. \tag{19}$$

For the purpose of elucidating the network dynamics, we found these *normal velocities* more useful to work with than the normal coordinates themselves for two reasons. First, from a computational point of view, it is easier to construct

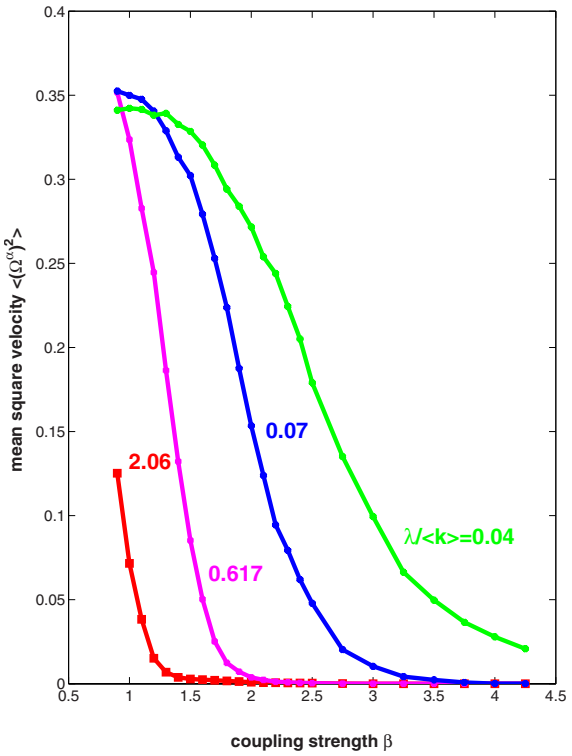

FIG. 11. (Color online): Plots of selected mean square normal velocities $\langle(\Omega^\alpha)^2\rangle_\omega$ as functions of coupling strength β averaged over 300 time units and 100 realizations of the intrinsic frequencies ω, for a single highly clustered Poisson network. Each curve is labeled with the scaled eigenvalue corresponding to α. The two lowest (and farthest left) curves correspond to eigenvalues at the high and low ends of the main spectral peak, while the other two curves are for modes within the low-lying second peak of "community" modes. The different velocity components drop to zero at different rates, and ones corresponding to high eigenvalues lock (or drop to zero) at lower coupling strengths.

time averages of the velocities as one requires only initial and final phases (not modulo 2π for this purpose) together with the elapsed time. Second, we found that plots of the velocities as functions of coupling strength displayed sharper transitions and clearer patterns than averages (or mean squares) of coordinates.

Figure 11 shows plots of the mean square velocities $\langle(\Omega^\alpha)^2\rangle$ as functions of coupling strength β for four different values of α taken from different parts of the spectrum for a highly clsutered Poisson network. The time averages Ω^α were taken over an interval of 300 time units and the squares were averaged over 100 realizations of the random frequencies. The different $\langle(\Omega^\alpha)^2\rangle$ values fall to zero at different rates, so that the eigendirections associated with high eigenvalues become locked (i.e., the corresponding velocities become zero) at lower values of β than the ones associated with low eigenvalues. Similar trends were noted for SFNs in [19]. The normal velocites give more detailed information about synchronization than a global order parameter. The evolution with increasing β from complete incoherence to complete frequency synchronization can be visualized as a series of quasi-independent locking transitions in which different normal modes effectively drop out of the active dynamics. As eigendirections successively lock, the phase space of the oscillator system can be viewed as contracting onto progressively lower-dimensional subspaces spanned by the remaining eigenvectors. Modes with very low eigenvalues are very difficult to lock, and therefore their presence will inhibit complete synchronization. Evidently these low modes are correlated with the difficulty of full synchronization in highly clustered networks.

To the extent that the modes behave as independent degrees of freedom, one can view each mode as having its own individual transition point, a critical coupling strength above which that mode is locked. To obtain numerical estimates of these individual transitions, we considered a mode to be locked when the value of $\langle(\Omega^\alpha)^2\rangle$ falls below a threshold of 0.01. (Since we are measuring an average over frequency realizations, this means that for the majority of realizations the value of Ω^α is actually zero within the resolution of our numerical measurement.) Frequencies were measured at a sequence of values of β for one network of each of the types we studied. As in Fig. 11 the frequencies Ω^α were time averaged over 300 time units, and their squares were averaged over 100 realizations of the random intrinsic frequencies. The transition points β_c were estimated by means of a cubic spline interpolation of the numerical measurements. The results are plotted in Figs. 12 and 13. The patterns are somewhat different for each type of network, but as a general rule β_c is a decreasing function of the eigenvalue λ. In some of the networks, a finite subset of the modes all lock at the same β value while the remainder lock and unlock independently. Evidently, some modes are strongly mutually coupled while others are more independent. For the strongly clustered SFN, for example, it is evident from Fig. 12 that a number of high modes lock simultaneously at a quite low value of β=0.5. This group of modes apparently represents the degrees of freedom responsible for the advanced partial synchronization of this network and the upward turn in the global order parameter seen in Fig. 10. For the normalized networks, all modes within the main spectral peak lock almost simultaneously, and only the lower set of modes (in highly clustered networks) have significant spread in their values of β_c. The low-eigenvalue modes that form at high clustering are difficult to lock, and it is evidently these modes that are responsible for the inhibition of complete synchronization in the cases of highly clustered neworks. Since these modes are associated with the divisions among communities, this suggests that the frequency clusters noted at moderately high β in [31] are identical to topological communities. The degrees of freedom that inhibit full synchronization are clearly different from the ones responsible for the advanced partial synchronization of SFNs.

VI. CONCLUSIONS

We have examined the Laplacian spectra for several types of complex networks, seeing the effects on the spectra of degree distribution, clustering, and of coupling scheme (in particular, equal and bidirectional couplings versus input normalization). We found that increasing clustering has two

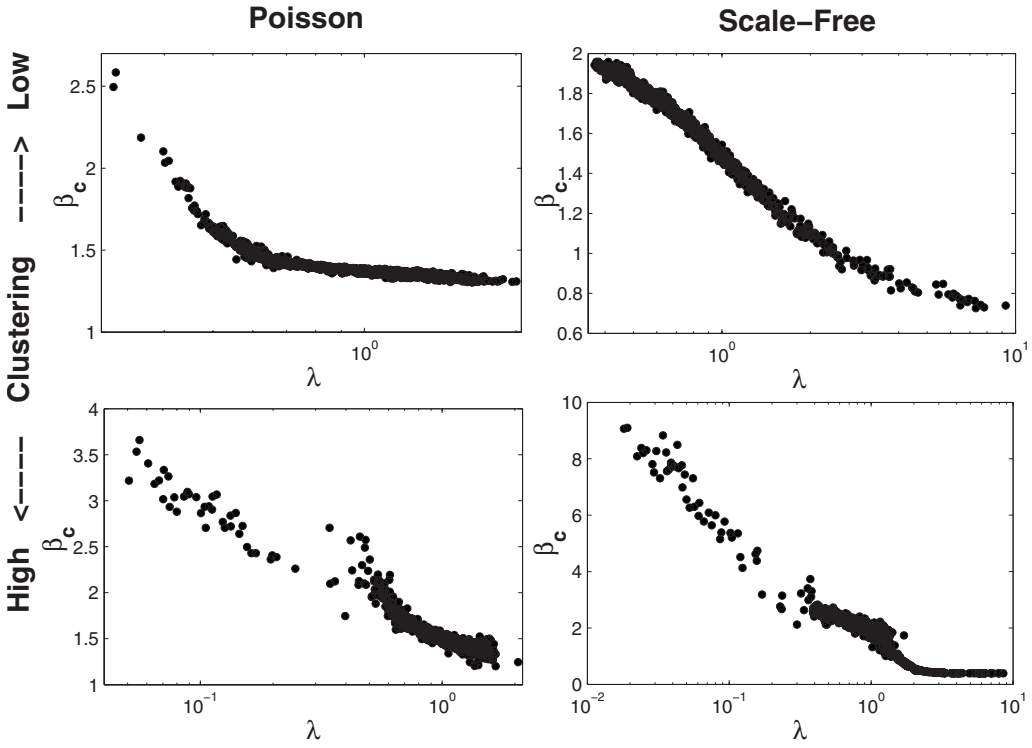

FIG. 12. Transition points β_c for individual eigenvectors of unnormalized networks. β_c is the coupling strength at which each mode locks as defined by the criterion $\langle(\Omega^\alpha)^2\rangle < 0.01$. Eigenvalues are plotted on a logarithmic scale in order to reveal the trend at low eigenvalues.

main groups of effects on the eigenvalue spectrum. The first set of effects alter the shape and composition of the main spectral peak. More localized modes are formed in and around this peak, and the correlation between eigenvalue and degree expectation value generally becomes stronger. Second, increased clustering creates an additional group of delocalized low-eigenvalue modes which are associated with an increased modularity (community structure) of the network. As expected, input normalization greatly reduces the influence of degree heterogeneity compared to the unnormalized network, and this is reflected in a greater uniformity of the spectra. Normalization, however, does not significantly alter the effect of clustering on communities and the low modes associated with them.

The behavior of the tail of the eigenvalue distribution is determined mainly by the distribution of node intensities. For example, power-law degree distributions lead to power-law decays of eigenvalue distributions. Normalized networks, in which all intensities are unity, have eigenvalue distributions lacking tails. The upper tail of the eigenvalue distribution is affected very little by clustering, but other properties of the corresponding eigenvectors (such as their degree of localization) do change significantly with clustering.

In general, study of the Laplacian spectra and the properties of the eigenvectors reveals complex structures whose significance should be explored further in future work. Many qualitative features are independent of the average degree $\langle k\rangle$ but depend only on the type of topology and coupling scheme. Some peculiar details of the spectral shapes we have observed remain to be fully explained (see, for example, Figs. 6 and 9).

We found that when coordinates based on the Laplacian eigenbasis are used to examine the dynamics of a network of coupled phase oscillators, the transition to synchronization can be visualized in ways that are not apparent from global order parameters alone. Roughly speaking, extremal eigenvalues give information about the onset of synchronization or desynchronization, whereas the full spectrum is relevant to the full process of synchronization. In particular, in many cases, modes or groups of modes make quasi-independent transitions to synchronization as the coupling strength is increased, with low modes synchronizing at higher coupling strengths. The process of synchronization can be viewed as a contraction of the dynamics onto progressively lower-dimensional submanifolds of the phase space as different eigenmodes lock one by one. The presence of low-lying modes, which are hard to lock, can significantly retard the achievement of full synchronization. The quasi-independence of eigenvectors is a somewhat surprising result in a highly nonlinear regime of partial synchronization. Previously the Laplacian was applied only to the linear stability of a perfectly synchronized state.

Unlike the situation with the linear (MSF) problem, in the regime of partial synchronization knowledge of the eigenvalue spectrum alone is not sufficient to predict the full dynamics. The dependence of transition point on eigenvalue is different for each type of network even though the broad trend (the transition point is a decreasing function of eigenvalue) is the same for all; but the spectrum is nonetheless a source of at least heuristic insight into the dynamics, and particular groups of eigenvectors can be directly associated with aspects of the dynamics: for example, high modes with the advanced transition in high-clustering SFNs, or low

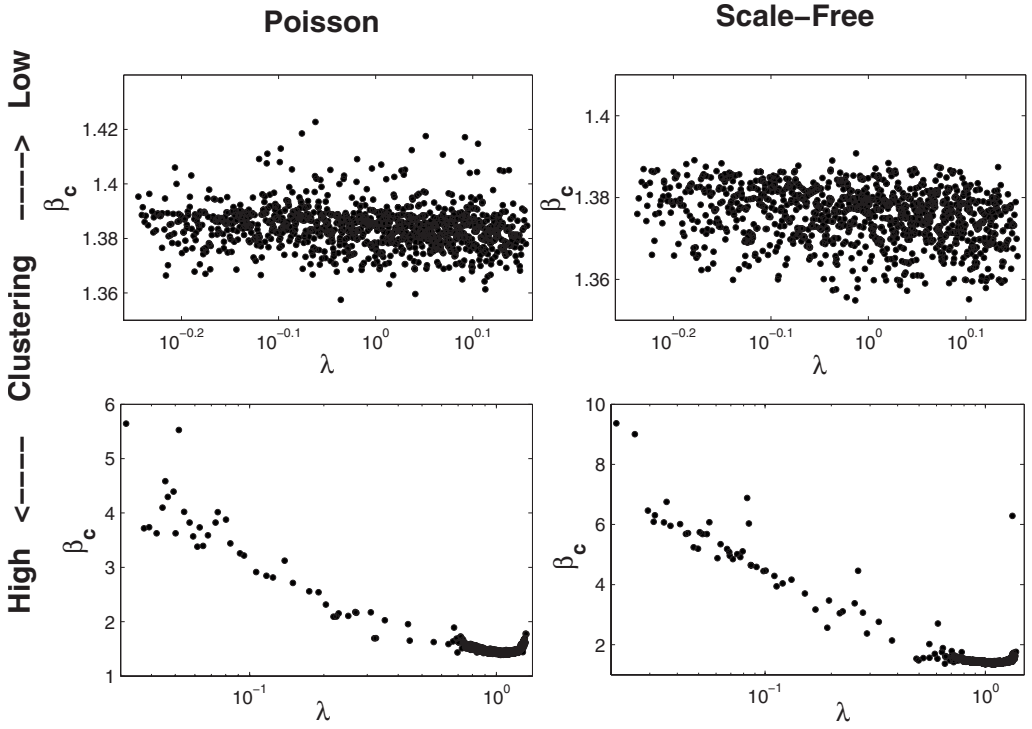

FIG. 13. Mode transition points β_c for normalized networks.

modes with frequency clustering and the inhibition of full synchronization.

In the future, diagnostic techniques based on the Laplacian spectrum can be applied to other types of networks. It may be worthwhile to examine spectral effects of assortative mixing, and to test our conjecture that assortative mixing should bring the Laplacian and adjacency matrix spectra into closer congruence. It may also be interesting to attempt a finite size scaling analyis of the separate transitions undergone by different normal modes. Just as one gains important information by considering the full process of synchronization and not only the onset [39], one also gains information by examining the full spectrum of eigenvectors.

ACKNOWLEDGMENTS

This work was supported by the NSERC of Canada.

[1] S. H. Strogatz, Nature (London) **410**, 268 (2001).
[2] R. Albert and A. L. Barabasi, Rev. Mod. Phys. **74**, 47 (2002); M. E. J. Newman, e-print arXiv:cond-mat/0202208; A. L. Barabasi, *Linked: The New Science of Networks* (Perseus Publishing, Cambridge, MA, 2002).
[3] M. E. J. Newman, SIAM Rev. **45**, 167 (2003); S. Boccaletti, V. Latora, Y. Moreno, M. Chavez, and D.-U. Hwang, Phys. Rep. **424**, 175 (2006).
[4] D. J. Watts, *Small Worlds* (Princeton University Press, Princeton, NJ, 1999); *Six Degrees* (Norton, New York, 2003).
[5] S. Wasserman and K. Faust, *Social Networks Analysis* (Cambridge University Press, Cambridge, England, 1994).
[6] D. J. Watts and S. H. Strogatz, Nature (London) **393**, 440 (1998).
[7] M. E. J. Newman and M. Girvan, Phys. Rev. E **69**, 026113 (2004).
[8] R. Albert, H. Jeong, and A. L. Barabasi, Nature (London) **406**, 378 (2000).
[9] R. Pastor-Satorras and A. Vespignani, Phys. Rev. Lett. **86**, 3200 (2001); Phys. Rev. E **63**, 066117 (2001).
[10] S. H. Strogatz, *Sync: The Emerging Science of Spontaneous Order* (Hyperion, New York, 2003).
[11] Y. Kuramoto, *Chemical Oscillations, Waves and Turbulence* (Springer-Verlag, Berlin, 1984); A. Pikovsky, *Synchronization* (Cambridge University Press, Cambridge, England, 2001).
[12] L. M. Pecora and T. L. Carroll, Phys. Rev. Lett. **80**, 2109 (1998).
[13] J. G. Restrepo, E. Ott, and B. R. Hunt, Phys. Rev. E **71**, 036151 (2005); Chaos **16**, 015107 (2005).
[14] N. Biggs, *Algebraic Graph Theory* (Cambridge University Press, London, 1974).
[15] B. Mohar, in *Graph Theory, Combinatorics and Applications*, edited by Y. Alavi, G. Chartrand, O. R. Ollermann, and A. J. Schwenk (Wiley, New York, 1991), pp. 871–898.
[16] F. Chung, *Spectral Graph Theory* (American Mathematical Society, Providence, RI, 1997).
[17] F. Chung, L. Lu, and V. Vu, Proc. Natl. Acad. Sci. U.S.A. **100**, 6313 (2003).

[18] A. Arenas, A. Diaz-Guilera, and C. J. Perez-Vicente, Physica D **224**, 27 (2006).
[19] P. N. McGraw and M. Menzinger, Phys. Rev. E **75**, 027104 (2007).
[20] K.-I. Goh, B. Kahng, and D. Kim, Phys. Rev. E **64**, 051903 (2001).
[21] I. J. Farkas, I. Derenyi, A. L. Barabasi, and T. Vicsek, Phys. Rev. E **64**, 026704 (2001).
[22] S. N. Dorogovtsev, A. V. Goltsev, J. F. F. Mendes, and A. N. Samukhin, Phys. Rev. E **68**, 046109 (2003).
[23] G. Biroli and R. Monasson, J. Phys. A **32**, L255 (1999).
[24] R. Monasson, Eur. Phys. J. B **12**, 555 (1999).
[25] A. E. Motter, C. S. Zhou, and J. Kurths, Europhys. Lett. **69**, 334 (2005); Phys. Rev. E **71**, 016116 (2005).
[26] C. Zhou, A. E. Motter, and J. Kurths, Phys. Rev. Lett. **96**, 034101 (2006).
[27] M. E. J. Newman, Phys. Rev. Lett. **89**, 208701 (2002).
[28] P. Erdős and A. Renyi, Publ. Math. (Debrecen) **6**, 290 (1959); Publ. Math., Inst. Hung. Acad. Sci. **5**, 17 (1960); Bull. Inst. Int. Stat. **38**, 343 (1961).
[29] A. L. Barabasi and R. Albert, Science **286**, 509 (1999).
[30] F. Chung and L. Lu, Proc. Natl. Acad. Sci. U.S.A. **99**, 15879 (2002).
[31] P. N. McGraw and M. Menzinger, Phys. Rev. E **72**, 026210 (2005).
[32] B. J. Kim, Phys. Rev. E **69**, 045101(R) (2004).
[33] C. Borgs, J. T. Chayes, M. Mahdian, and A. Saberi, Proceedings of the 10th ACM SIGKDD International Conference on Knowledge, Discovery and Data Mining (Association for Computing Machinery, New York, 2004); M. Fiedler, Czech. Math. J. **23**, 298 (1973); A. Pothen, H. Simon, and K.-P. Liou, SIAM J. Matrix Anal. Appl. **11**, 430 (1990); R. Kannan, S. Vempala, and A. Vetta, J. ACM **51**, 497 (2004); X. He, C. H. Q. Ding, H. Zha, and H. D. Simon, *Proceedings of the IEEE International Conference on Data Mining* (IEEE, New York, 2001), p. 195; C. H. Q. Ding, X. He, and H. Zha, *Proceedings of the 7th International Conference on Knowledge Discovery and Data Mining* (Association for Computing Machinery, New York, 2001), p. 275.
[34] L. Donetti and M. A. Muñoz, J. Stat. Mech.:Theor. Exp. (2004) P10012; e-print arXiv:physics/0504059, Proceedings of the 8th Granada Seminar—Computational and Statistical Physics (to be published).
[35] A. Capocci, V. D. P. Servedio, G. Caldarelli, and F. Colaiori, Physica A **352**, 669 (2005).
[36] E. P. Wigner, Ann. Math. **62**, 548 (1955); **65**, 203 (1957); **67**, 325 (1958).
[37] T. Guhr, A. Müller-Groeling, and H. A. Weidenmüller, Phys. Rep. **299**, 189 (1998).
[38] Y. Moreno and A. F. Pacheco, Europhys. Lett. **68**, 603 (2004).
[39] J. Gomez-Gardenes and Y. Moreno, e-print arXiv:cond-mat/0608309, Int. J. Bifurcation Chaos (to be published).
[40] Another procedure is necessary in cases where $\langle k \rangle$ is not well-defined, such as the thermodynamic limit of scale-free networks with small power-law exponents.